Proceedings of the
2007 IEEE Intelligent Vehicles Symposium
Istanbul, Turkey, June 13-15, 2007

A New Vehicle Detection with Distance Estimation for Lane Change Warning Systems

Bing-Fei Wu, Wei-Hsin Chen, Chai-Wei Chang, Chao-Jung Chen and Ming-Wei Chung

***Abstract*—In this paper, the vehicle detection with distance estimation algorithm is proposed by using two CCD cameras mounted on the both side mirrors of our experimental car, TAIWAN *i*TS-1. The Sobel edge pixels and gray intensity are applied for the lane marking and vehicle detection in our work. A new detection which utilizes a lane prediction technique to reduce the size of the ROI is developed for real-time embedded system applications. The side vehicles can be easily detected by comparing the gray intensity with the road surface. Then, the image coordinate model is utilized for the distance estimation with the detected approaching vehicles. The verified effective distance is 30m behind the host vehicle. This approach has been successfully implemented on the DSP board for the real-time detection and this system will be extended to the lane change warning system to give drivers alerts to avoid collision.**

I. Introduction

In recent year, an important issue of our daily life is the traffic safety. Thousands people died or got hurt in the road accidents, which are a major concern in developing countries. In order to keep the safety of drivers and passengers, the seatbelt and airbag are the necessary equipments of a vehicle. In fact, preventing methods are more important than the protecting equipments. A real-time vision-based system plays an important role for providing effective information like the lane marking, the front and side images, lane departure and distance with other vehicles. Therefore, the lane departure warning system, lane changing assistant system, blind spot detection system and preventing bumping system are the main applications of a real-time vision based safety driving system. There are two important issues for vehicle safety to be solved: lane marking detection and vehicle detection.

Some systems utilize radars to perform vehicle detection and blind spot detection. Valeo Raytheon system [1] using a 24-GHz radar sensor to monitor the blind spot at the two sides on the host vehicle. The sensors were embedded into the back side bumper of the host vehicle and the detection range is 150° within 40m. If there are some vehicles in the blind spot, there would be a vision warning signal to caution the driver. The Visteon system [2] is also a radar based one which uses a 24-GHz radar with 6m detection range. The detection region is programmable and the system will not warn while detecting the static object like telegraph pole.

There are many algorithms for detecting the lane marking on the road [3][4][5]. Song and Tai [6] utilized the image processing technique to locate the lane marking position. The feature of lane marking is a long straight line and every lane marking line is intersected to each other near the vanishing point. Krips, Velten and Kummert[7] applied the shadow based classification algorithm, and the adaptive template matching method to detect the vehicles. The method is characterized by the self adjusted template and the matching score that allows false target rejection. In [8], a set of sensors including far radar, stereo vision system and side radar are set up for monitoring the left side of the vehicle. All sensors are connected via CAN-Bus to a PC and deliver CAN messages with object coordinates relative to the specific sensor. In [9], the optical flow based obstacle detection system is developed in detecting vehicles approaching the blind spot of a car. They utilize inverse perspective mapping to predict and find an edge pixel in 3×3 neighborhood of the next image to detect obstacle. In [10], the approach is based on motion and on a lane-based projection of the camera image. It detects vehicle motions like leaving, approaching or static objects at every frame.

In this paper, the vehicle detection with distance estimation is proposed by using two CCD cameras mounted on the both side mirrors of our experimental car, TAIWAN *i*TS-1 in Fig. 1. As shown in Fig. 2, the CCD cameras are on the top of both side mirrors with 6mm focal length. The Sobel edge pixels and gray intensity are applied for the lane marking and vehicle detection approaches. The vehicle can be detected by comparing the gray intensity with the road surface. Then, the image coordinate model is utilized for the distance estimation with the detected approaching vehicles. The verified effective distance is 30m behind the host vehicle. Finally, this approach also has been implemented successfully on the DSP board in Fig. 3 for the real-time detection and this system will be extended to the lane change warning system to give drivers alerts to avoid collision.

This paper is organized as follows: Section II presents the proposed algorithm including the lane marking detection, vehicle detection and distance estimation. Section III addresses the experimental results of the vehicle detection and distance estimation. The conclusion and future work are given in Section IV.

B.-F. Wu, W.-H. Chen, C.-W. Chang, C.-J. Chen and M.-W. Chung are all with the Department of Electrical and Control Engineering, National Chiao Tung University, Hsinchu, Taiwan, R.O.C. (e-mail: bwu@cc.nctu.edu.tw)

1-4244-1068-1/07/$25.00 ©2007 IEEE.

Fig. 1. TAIWAN *i*TS-1.

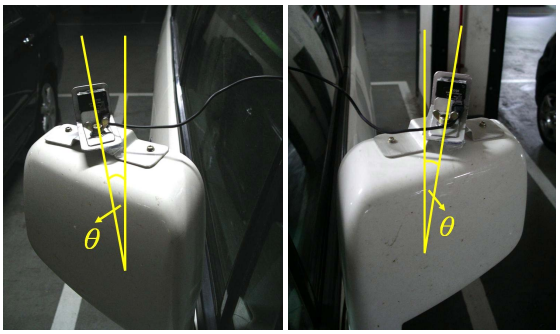

Fig. 2. The CCD cameras on the two side view mirrors.

Fig. 3. TI TMS320DM642 DSP board.

II. Detection Algorithm

In our system, the height of the camera is 1.2m and the pan angle, θ, between the camera and the vehicle in Fig. 3 is 16° and the captured images are shown, respectively, in Fig. 4. The flow chart of the proposed lane marking and vehicles detection algorithm is illustrated in Fig.5. Firstly, the near lane marking is detected. Secondly, the neighboring lane whether there are closing vehicles or not will be identified. If there is no closing vehicle in the neighboring lane, the adaptive region of interest (ROI) is set and detecting the far lane marking in the adaptive ROI. If there are vehicles in the neighboring lane, the lane marking will be covered and the far lane marking by the information of the near lane marking is predicted. Finally, the approaching vehicles are detected and the distance away from the host vehicle is also estimated.

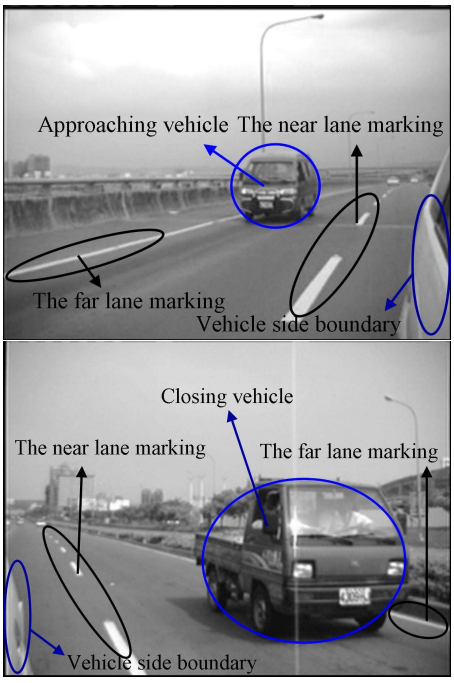

Fig. 4. The captured image by the CCD camera.

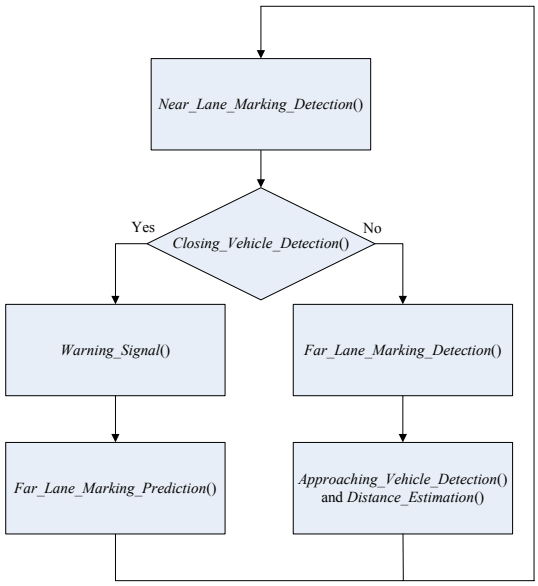

Fig. 5. The flow chart of lane marking and vehicle detection algorithm.

The proposed algorithm is only implemented in the bottom half image, since the main lane information only appear in the bottom image. The two 3×3 Sobel masks illustrated in Fig. 6 are applied to obtain the horizontal and vertical edge pixels of the image. The detected edge pixels of horizontal and vertical masks are shown in Fig. 7, and the edge pixels are denoted as white points.

1	2	1
0	0	0
-1	-2	-1

(a)

1	0	-1
2	0	-2
1	0	-1

(b)

Fig. 6. (a) The horizontal sobel mask. (b) The vertical sobel mask.

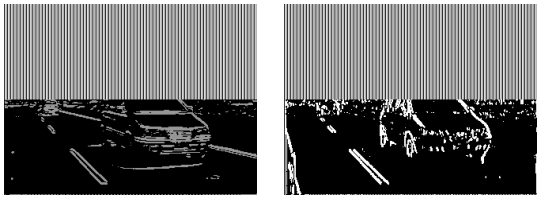

(a) (b)

Fig. 7. (a) The horizontal Sobel edge pixels. (b) The vertical Sobel edge pixels.

A. Near Lane Marking Detection

In the beginning of the detection, two modes, Single Mode and Continuous Mode, for the ROI determination are defined for the near lane marking detection. As shown in Fig. 8, a wider ROI in Single Mode is assigned than that in Continuous Mode. Single Mode starts if there is no previous near lane information for referring, i.e. the near lane marking is not detected in the previous image. Otherwise, the narrow ROI is given for detection to reduce the computing consumption. Note that the detection starts from Single Mode. The mode will not switch to Continuous Mode until the near lane is detected. When the near lane information is obtained, Continuous Mode enables. Once the process misses the near lane information, Single Mode will be restarted. The ROI in Single Mode is labeled as the ABCD area in Fig. 8 and that in Continuous Mode is bounded in PQRS area in Fig.9.

Fig. 8. The ROI in Single Mode.

Fig. 9. The ROI in Continuous Mode.

In the ROI, near lane marking is figured out by the vertical edge pixels and gray intensity. L and R in Fig.10(a) are located at the points, if $Edge_L$ is true , $Edge_R$ is true , $\bar{I}_{\overline{LR}} > I_{R+5}$ and $\bar{I}_{\overline{LR}} > I_{L-5}$ where $Edge_L$ and $Edge_R$ are the edge pixels of L and R, I means the gray intensity of the pixel and $\bar{I}_{\overline{LR}}$ indicates the average gray intensity within $\overline{LR}$.

The lane marking is represented as M_i in the i^{th} scan line with (u_i, v_i) on the image plane. The lane marking is detected row by row from the bottom to the top in the ROI. The pixels of M set is described as a straight line by $v = a_0 + a_1 u$, where a_0 and a_1 are obtained by least square method from (1), where N means amount of the detected lane marking pixels.

$$\begin{bmatrix} N & \sum u_i \\ \sum u_i & \sum u_i^2 \end{bmatrix} \begin{bmatrix} a_0 \\ a_1 \end{bmatrix} = \begin{bmatrix} \sum v_i \\ \sum u_i v_i \end{bmatrix} \quad (1)$$

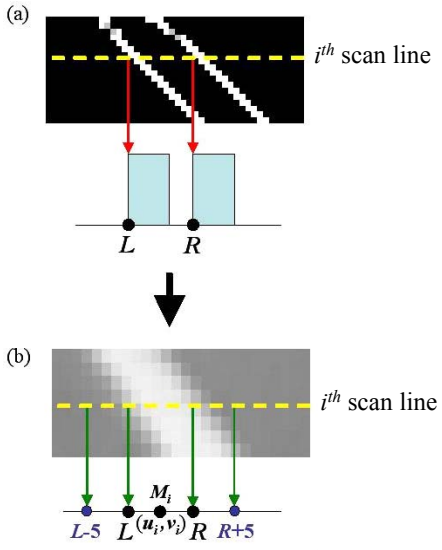

Fig. 10. (a)Sobel edge detection. (b)Lane marking determination.

B. Closing Vehicle in the neighboring lane detection

When there is a closing vehicle in the neighboring lane, a huge amount of gray intensity that is different with the road will appear. Therefore, an RH area is arranged as Fig. 11 to estimate the gray intensity histogram of the road surface. In order to avoid the influence of the white lane marking, we set RH_Width > RH_Height . The gray intensity histogram is shown in Fig. 12. The largest number of gray intensity is denoted as $I_{RH_{\max}}$ and the region $R \in \left[I_{RH_{\max}} - 30,\ I_{RH_{\max}} + 30 \right]$ is assigned as the gray intensity region of the road surface. The gray intensity of the pixels, $I(u,v)$, in LV_1 and LV_2 will be check with R and the ratio, $\rho = P/N$, is obtained, where P indicates the amount of the pixels where $I(u,v) \notin R$ and N means the total pixels in LV_1 and LV_2 respectively. In case of $\rho_{LV_1} > 0.8$ or $\rho_{LV_2} > 0.8$, it implies that there is a closing vehicle in the neighboring lane.

Fig. 11. The check region of vehicle detection in the neighboring lane.

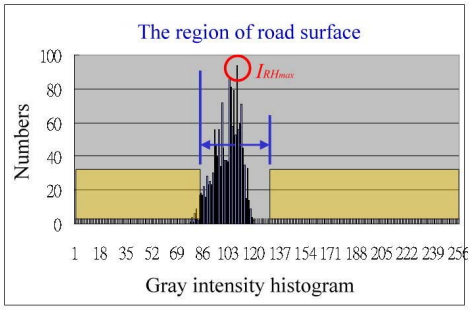

Fig. 12. The gray intensity histogram of *RH* area.

C. Far Lane Marking Detection and Approaching Vehicle Detection and Distance Estimation

If there is no closing vehicle in the neighboring lane, then the far lane marking detection starts. The ROI of the far lane marking is set up by the detected near lane marking in Fig .13. In Section B, the near lane marking straight line is described as $v = a_0 + a_1 u$. It is assumed that the lane width is always the same and is denoted as *W*. (2) and (3) represent the projection relationship form the world space (X_r, Y_r, Z_r) to the image plane (u, v), where H means the height of the camera, e_u and e_v are the intrinsic parameters of the camera and are denoted as (4) and (5). *du* and *dv* in (4) and (5) are the physical width and height, respectively, of an image pixel, where *f* is the focal length of the camera.

$$u = e_u \frac{X_r}{Y_r} \tag{2}$$

$$v = e_v \frac{m_\varphi \cdot Y_r - H}{Y_r} \tag{3}$$

$$e_u = \frac{f}{du} \tag{4}$$

$$e_v = \frac{f}{dv} \tag{5}$$

From (2), (3), (4) and (5) the lane width in world space, *W*, maps to the image plane and is shown as

$$\Delta u = \left(\frac{W}{H}\right)\left(\frac{e_u}{e_v}\right)\left(e_v m_\varphi - v\right)\sec\theta, \tag{6}$$

By (6), the ROI of the far lane marking can be set up as Fig.13. The straight line $v = a_2 + a_3 u$ of the predicted ROI can be obtained by the estimation of the horizontal distance in the image from the near lane marking to the far lane marking.

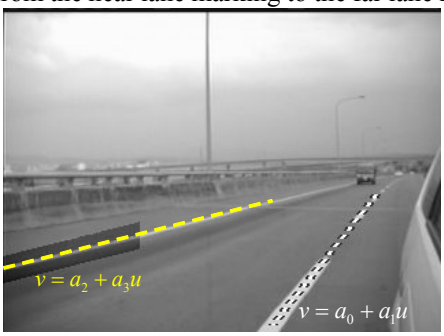

Fig. 13. Adaptive ROI of far lane marking.

In Fig. 14, the vanishing point A is at intersection of the two lane markings. Three virtual lines in the neighboring lane can be determined. M_1, M_2 and M_3 are the middle points of $\overline{BC}$, $\overline{BM_1}$ and $\overline{BM_2}$ respectively. If some horizontal edge pixels are detected on the three virtual lines, the density of horizontal edge pixels in D_hBox in Fig. 15 will be estimated.

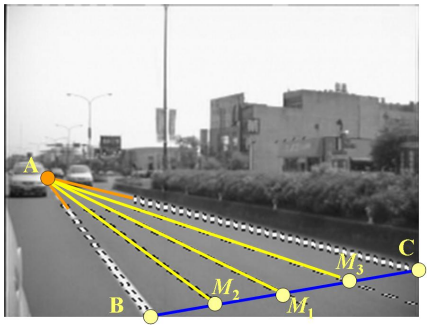

Fig. 14. The virtual lines in the neighboring lane.

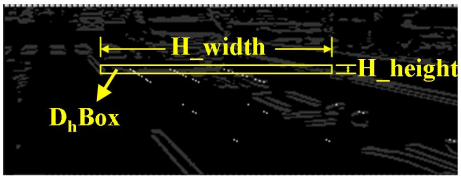

Fig. 15. The check region of horizontal edge pixels.

H_width is the width of the lane width and H_height is three pixels height If the density of horizontal edge pixels in D_hBox is large enough, the system starts to check the density of vertical edge pixels in D_vBox in Fig. 16. V_width is the width of the lane width and V_height is half of V_width. If the density of the vertical edge pixels in D_vBox is large enough, it implies that there exists a approaching vehicle in the neighboring lane. Fig. 17 shows the detection result, the white horizontal line means the bottom of the vehicle.

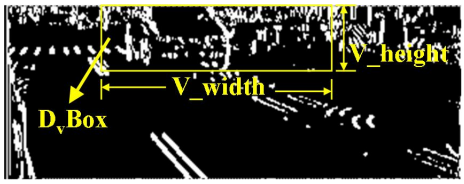

Fig. 16. The check region of vertical edges.

Fig. 17. The approaching vehicle detection results.

If the approaching vehicle is detected, the system will start to estimate the distance from the vehicle to the host vehicle. The real distance D from the detected vehicle to the host vehicle shown in Fig. 18 is estimated by cosine theorems, where D_{cv} means the distance between the detected vehicle and the camera, L indicates the distance from the side mirror to the back side of the vehicle.

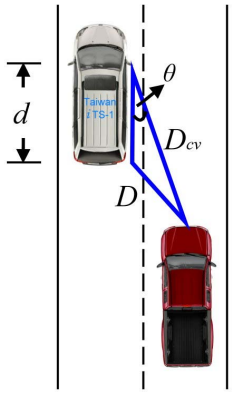

Fig. 18. The distance from detected vehicle to our system.

D. Warning Signal Generation and Far Lane marking Prediction

If there is a closing vehicle on the neighboring lane, the far lane marking is covered by the closing vehicle, so that it can not be detected. An LED will light up to caution the driver not to change lane avoiding crash and the system starts to predict the position of the covered lane marking. In our observation, the lane width is always a constant length for normal driving. From Section C, the far lane marking can be obtained as $v = a_2 + a_3 u$. In Fig. 19, the far lane marking is predicted since it is covered by the closing vehicle.

Fig. 19. The estimated far lane marking.

III. Experimental Results

The system has been built up on TAIWAN *i*TS-1. The recorded gray images from CCD cameras are transferred to the TMS320DM642 DSP board in 320×240 NTSC format. The experiment is established on the urban road and highway in Hsinchu, Taiwan. The estimated distance is in the left top of the output images, shown in Fig. 20 and Fig. 21 for urban road and highway, respectively. The results reveal that the proposed algorithm is not affected by the shadows or the marking on the road surface. The comparison of the real and estimated distances is summarized in Table I with the accuracy ratio.

TABLE I
DISTANCE ESTIMATION

Real Distance (m)	Estimated Distance (m)	Accuracy Ratio (%)
25.7	26.37	97.39
13.2	13.37	98.71
8.2	8.57	95.49
6.1	6.23	97.87
4.1	3.97	96.83

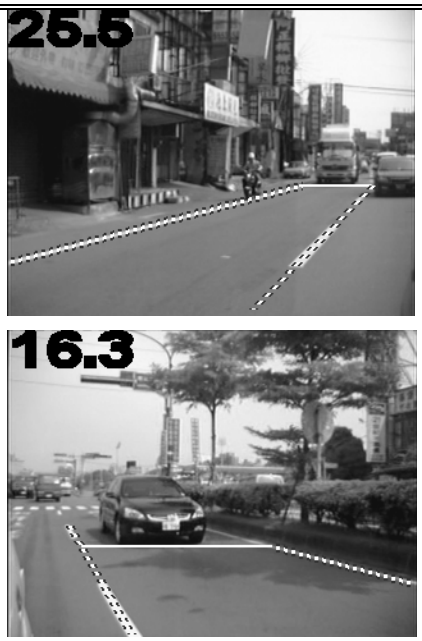

Fig. 20. The detection results for road.

Fig. 21. The detection results for highway.

IV. Conclusion and Future Work

In this paper, we have developed a new algorithm and implemented the system for vehicle detection of the neighboring lane. The system can detect the vehicle away from 30 m and is not affected by the shadows and marking on the road surface. The image processing time is quick enough for real-time application and the estimated vehicle distance are precise enough for avoiding collision.

Furthermore, the algorithm will be improved for motorcycle detection. The detection of motorcycles can prevent vehicle drivers to open the door when some motorcycles are close to the vehicle.

Acknowledgment

The work is supported by National Science Council under Grant no. NSC 95-2752-E-009 -012 -PAE.

References

[1] http://www.valeoraytheon.com/hazards.html, accessed Jan. 2007.
[2] http://www.visteon.com/products/automotive/driver_awareness.shtml, accessed Jan. 2007.
[3] S. Kamijo, Y. Matsushita, K. Ikeuchi, and M. Sakauchi, "Traffic monitoring and accident detection at intersections," *IEEE Trans. Intelligent Transportation Systems*, vol. 1, no. 2, pp. 108-118, Jun. 2000.
[4] C. Zhaoxue and S. Pengfei, "Efficient method for camera calibration in traffic scenes," *IEE Electronic Letter*, vol. 40, no. 6, pp. 368-369, Mar. 2004.
[5] A. H. S. Lai and N. H. C. Yung, "Lane detection by orientation and length discrimination," *IEEE Tran. System, Man, and Cybernetics, B, Cybernetics*, vol. 30, no. 4, pp. 539-548, Aug. 2000.
[6] K.-T. Song and J.-C. Tai, "Dynamic calibration of pan-tilt-zoom cameras for traffic monitoring," *IEEE Trans. Systems, Man, and Cybernetics, B, Cybernetics*, vol. 36, no. 5, pp. 1091-1103, Oct. 2006.
[7] M. Krips, J. Valten, A. Kummert, "AdTM tracking for blind spot collision avoidance," *in Proc. IEEE Intelligent Vehicles Symposium*, pp. 544-548, Jun. 2004.
[8] M. Rudar, W. Enkelmann and R. Garnitz, "Highway lane change assistant," in *Proc. IEEE Intelligent Vehicles Symposium*, vol. 1, pp. 204-244, Jun. 2002.
[9] P. H. Batavia, D. A. Pomerleau and C. E. Thorpe, "Overtaking vehicle detection using implicit optical flow," *in Proc. IEEE Conference on Intelligent Transportation System*, pp. 729-734, Nov. 1997.
[10] A. Techmer, "Real-time motion analysis for monitoring the rear and lateral road," *in Proc. IEEE Intelligent Vehicles Symposium*, pp. 704-709, Jun. 2004.